

Supramolecular assembly of phosphonate-substituted porphyrins in Langmuir layers and Langmuir-Schäfer films: structural studies and selective sensing of pyridine

Elizaveta V. Ermakova^{†,*}, *Vladimir V. Arslanov*[†], *Yann Bretonnière*[‡], *Carine Michel*[‡], *Alla Bessmertnykh-Lemeune*^{‡,*}.

[†]Frumkin Institute of Physical Chemistry and Electrochemistry, Russian Academy of Sciences, Leninsky Pr. 31-4, Moscow 119071, Russia.

[‡]Laboratoire de Chimie, UMR 5182, CNRS, ENS de Lyon, 46 allée d'Italie, CEDEX, 69364 Lyon, France

Supporting information

Table of Contents:

1. UV-vis and fluorescence spectroscopies studies	2
2. Fitting of <i>in situ</i> UV-vis spectra of H ₂ DPPP and H ₂ OPPP monolayers	3
3. Monolayers of H ₂ DPPP, H ₂ TPPP and H ₂ OPPP at the air-water interface	4
4. LS and drop-cast films of H ₂ OPPP	6
5. Acidochromism studies of H ₂ DPPP, H ₂ TPPP and H ₂ OPPP in chloroform solution..	8
6. Monolayers of NiOPPP and ZnOPPP at the air-water interface	9
7. LS films of NiOPPP and ZnOPPP	12
8. Monolayer and LS film of ZnTPP	14
9. UV-vis and fluorescence spectroscopies studies of ZnOPPP and ZnTPP in chloroform solutions in presence of amines	15
10. Quantum yield measurements for ZnOPPP LS film	17

1. UV-vis and fluorescence spectroscopies studies

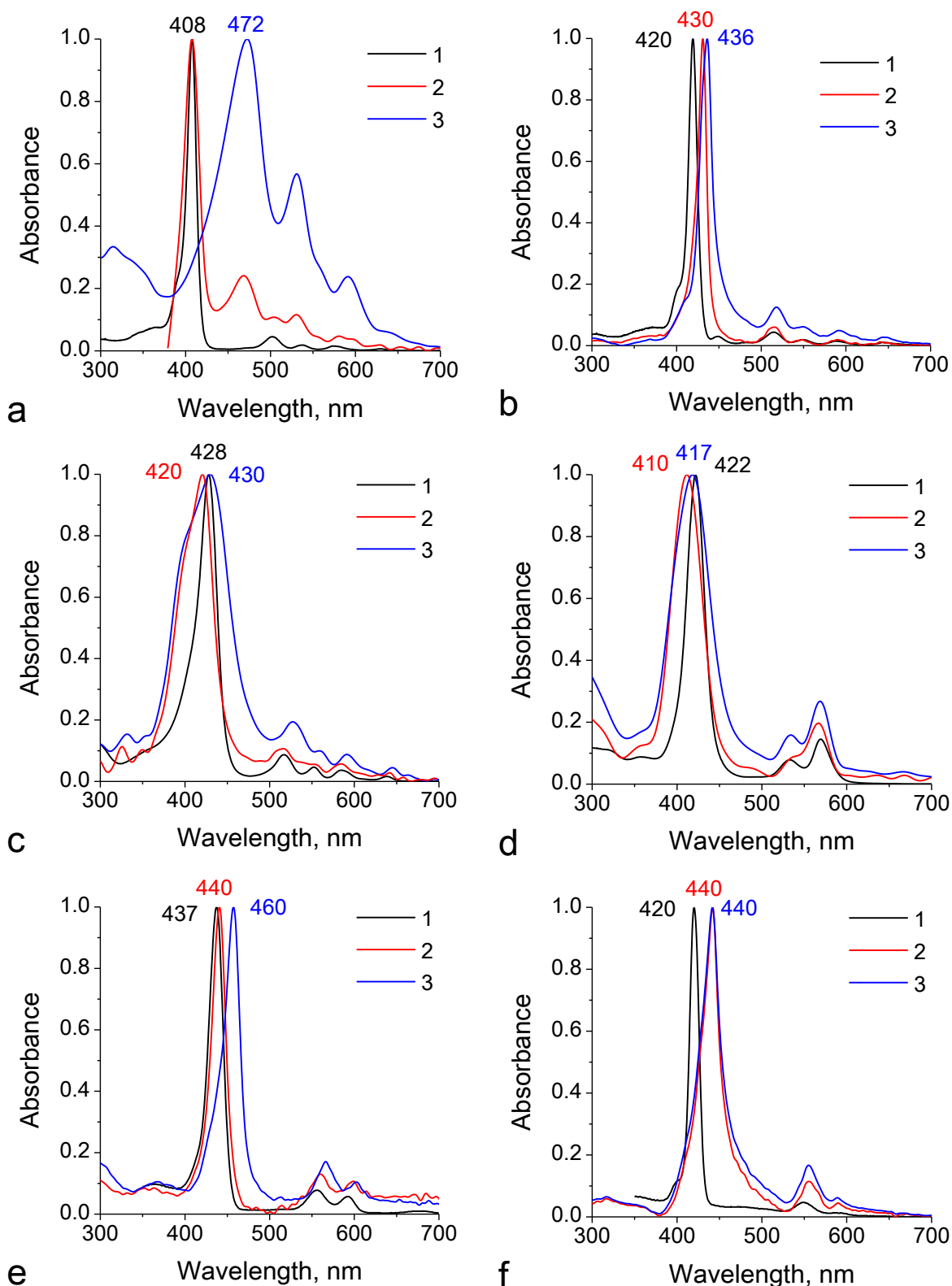


Figure S1. Normalized [0;1] UV-vis spectra of H₂DPPP (a), H₂TPPP (b) and H₂OPPP (c), NiOPPP (d), ZnOPPP (e), ZnTPP (f) in chloroform solution (1), monolayer on the deionized water at surface pressure 0 (2) and 35 (3, a), 18 (3, b), 22 (3, c), 35 (3, d), 30 (3, e), 24 (3, f), 27 (3, g) mN m⁻¹.

2. Fitting of *in situ* UV-vis spectra of H₂DPPP and H₂OPPP monolayers

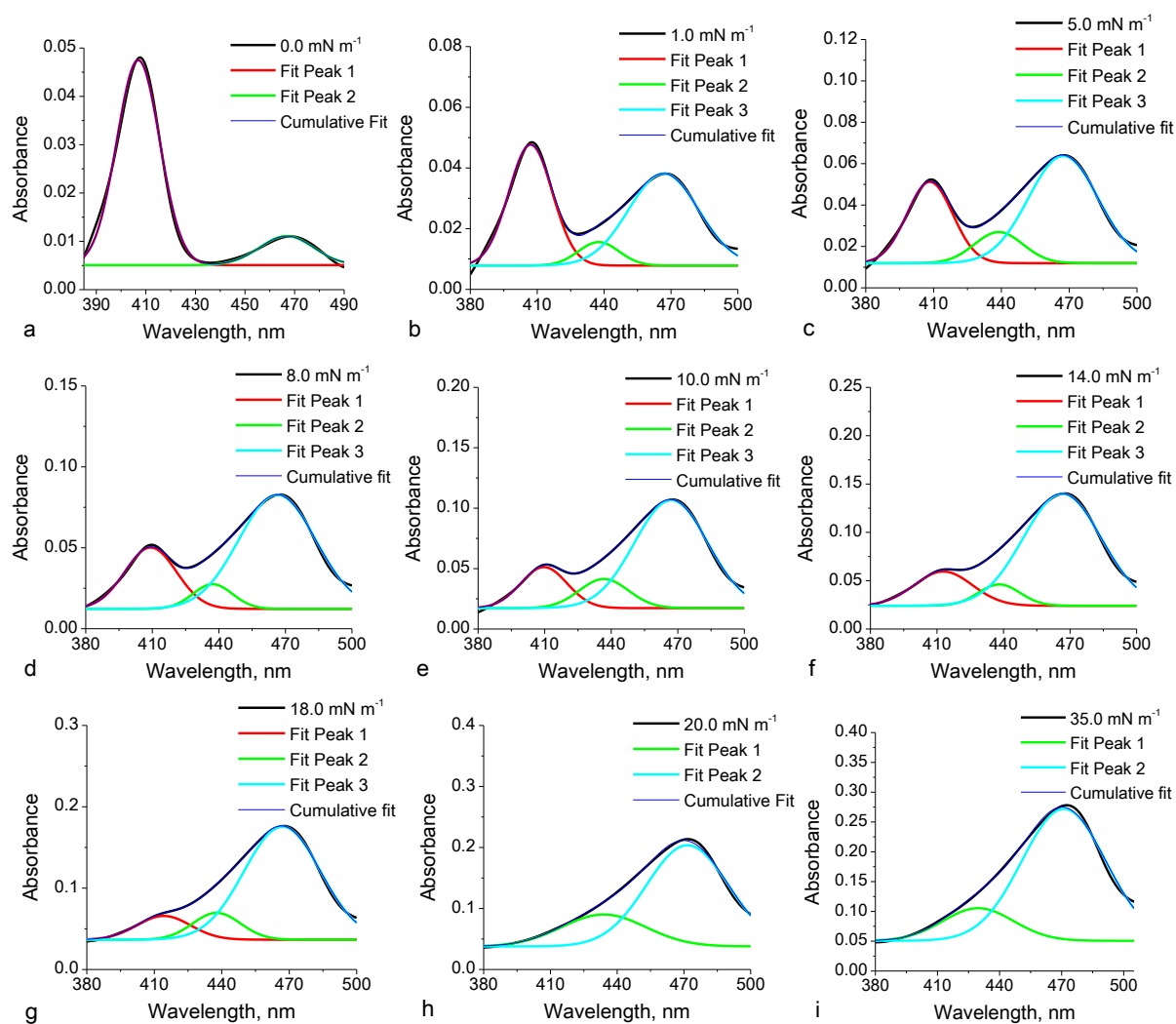
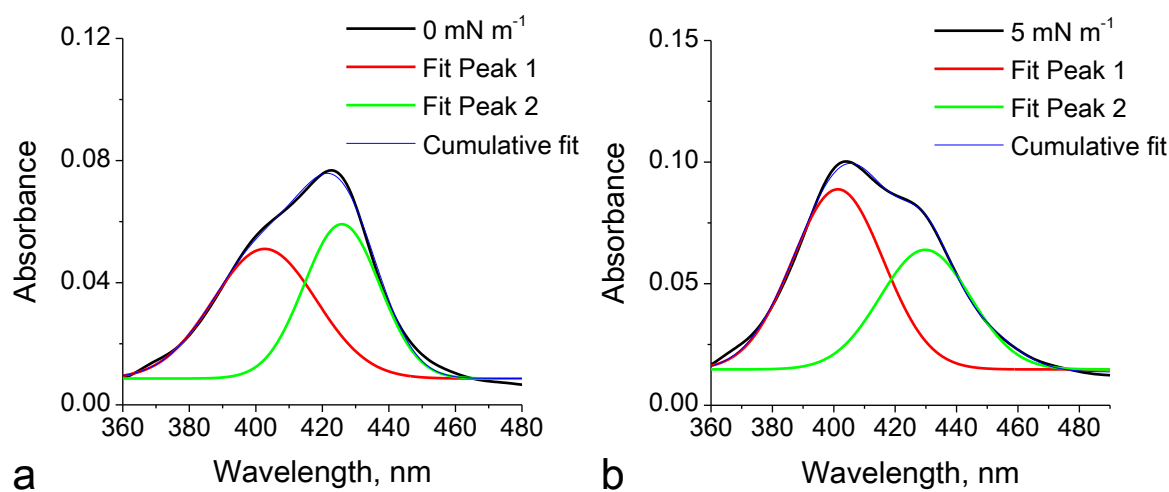


Figure S2. *In situ* UV-vis spectra of H₂DPPP monolayer and their multipeak Gaussian fitting.



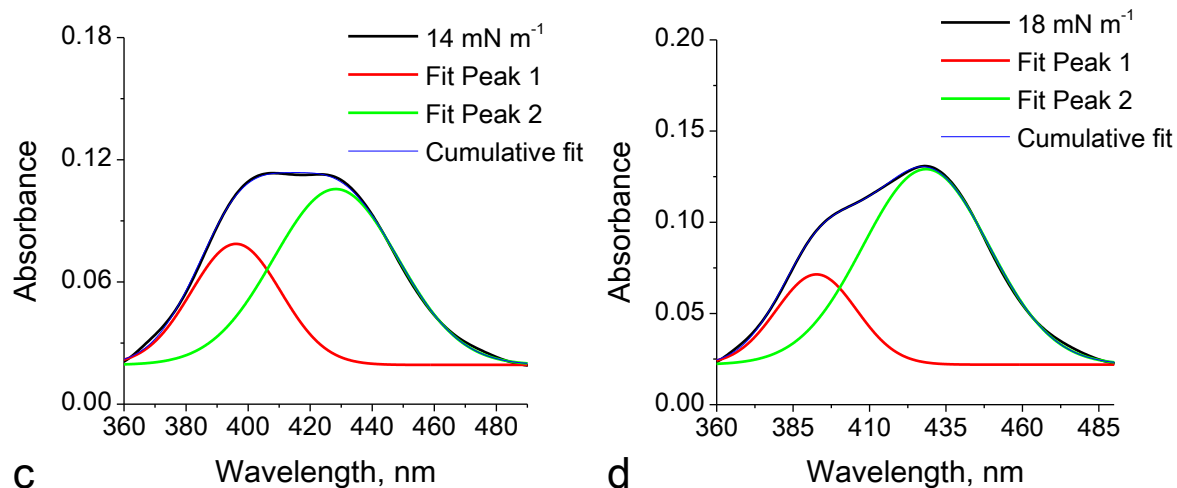


Figure S3. *In situ* UV-vis spectra of H₂OPPP monolayer and their multipeak Gaussian fitting.

3. Monolayers of H₂DPPP, H₂TPPP and H₂OPPP at the air-water interface

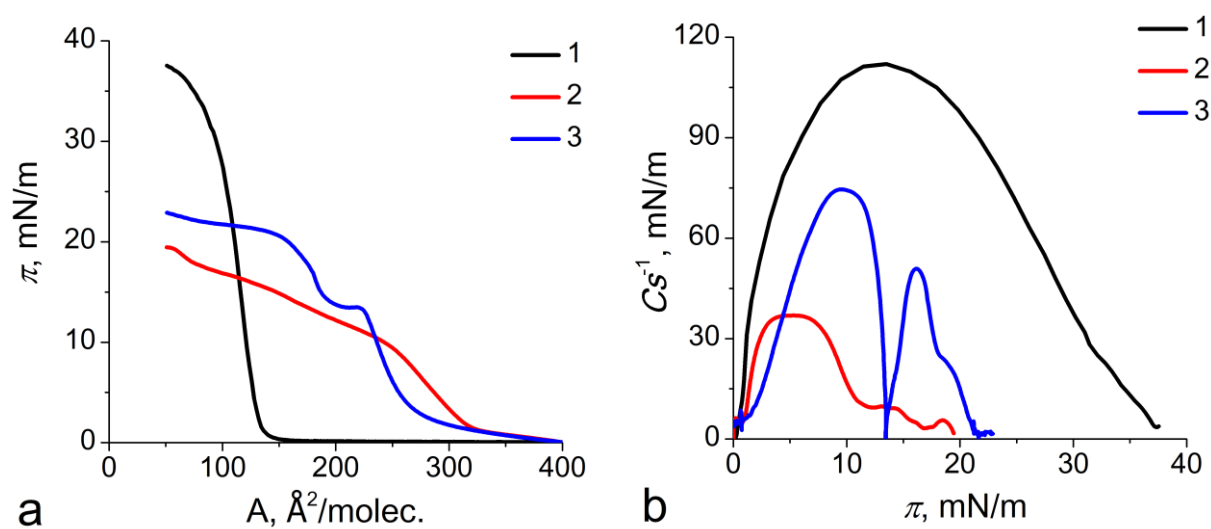


Figure S4. (a) Surface pressure–area isotherms and (b) compressibility modulus C_s^{-1} vs. surface pressure plots for the H₂DPPP (1), H₂TPPP (2) and H₂OPPP (3) monolayers on the water surface.

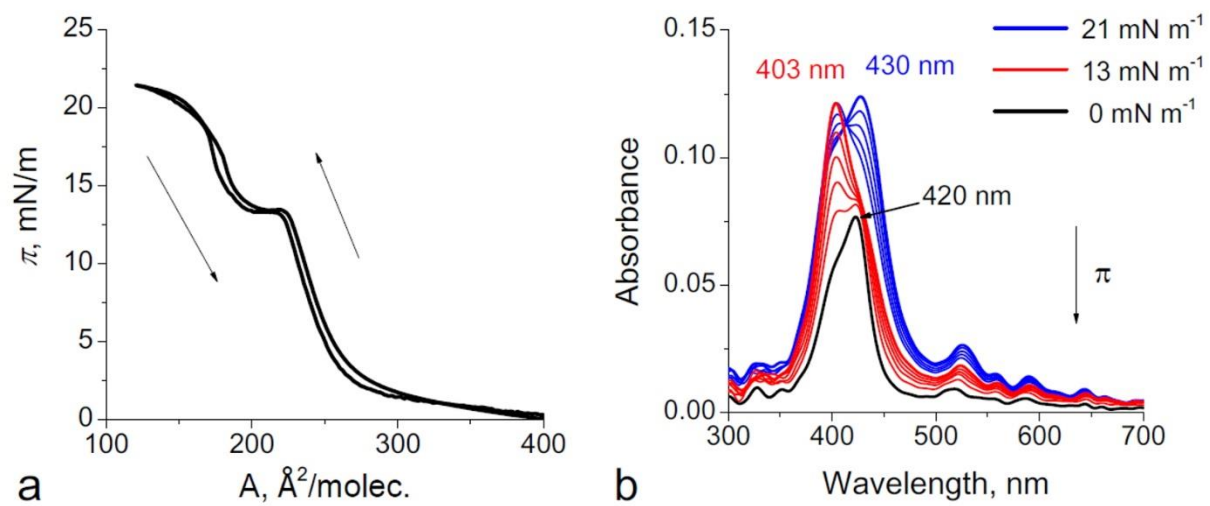


Figure S5. (a) Compression–expansion cycles for porphyrin H₂OPPP. (b) *In situ* UV–vis spectra of the H₂OPPP monolayer recorded during the monolayer expansion.

4. LS and drop-cast films of H₂OPPP

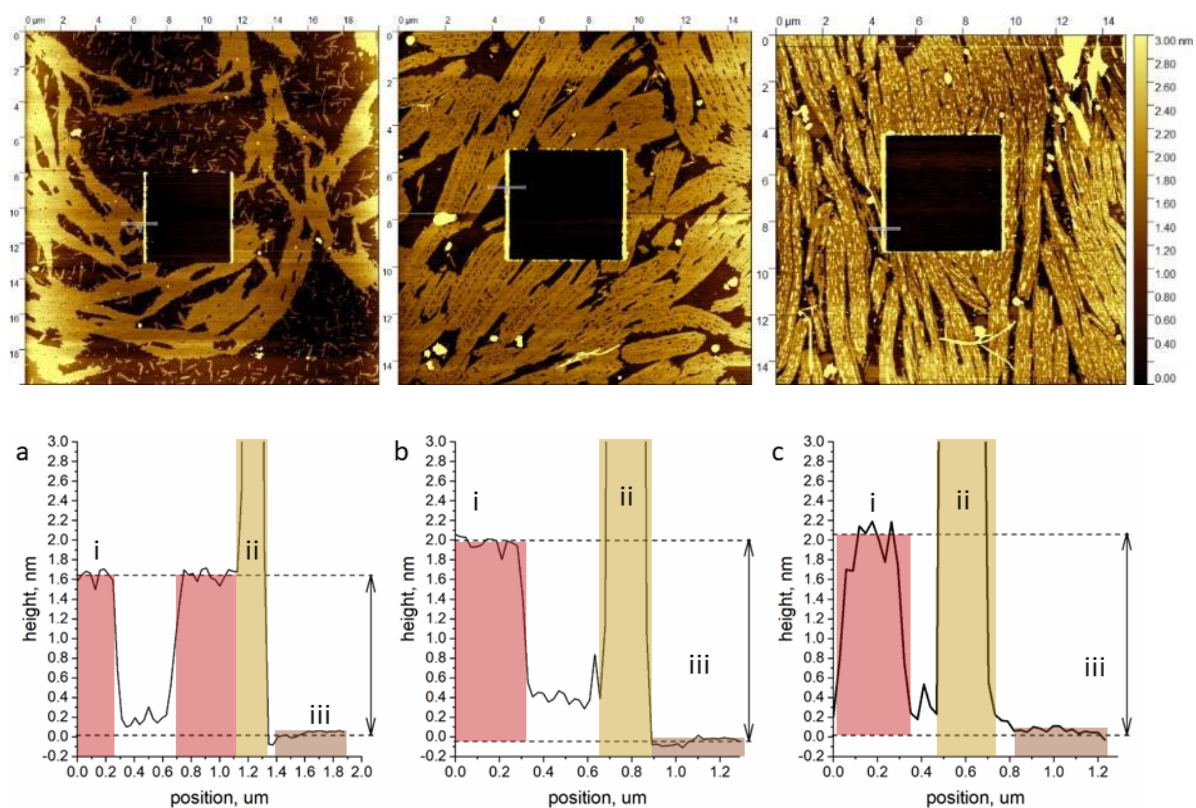


Figure S6. AFM images obtained after ‘scratching’ the samples in contact mode to reveal bare mica. Top, from left to right: LS film of H₂OPPP transferred onto mica at 5, 14, and 18 mN m⁻¹. Bottom: corresponding height profiles obtained along the scratched surface line for samples transferred at (a) 5, (b) 14, and (c) 18 mN m⁻¹. Colored regions on the height profiles correspond to (i) observed porphyrin domains, (ii) film material piled up after ‘scratching’, and (iii) bare mica surface.

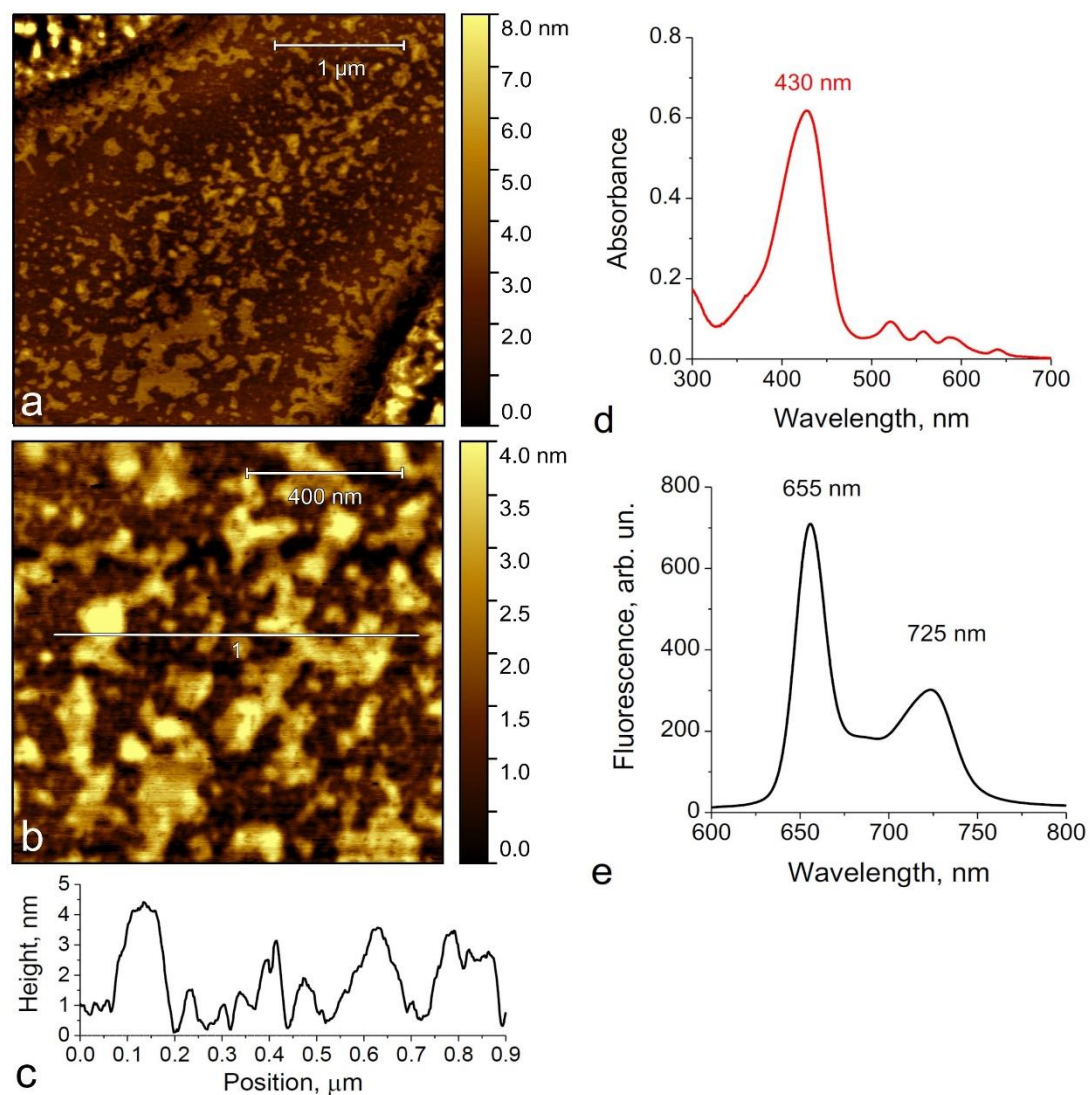


Figure S7. (a, b) AFM images of drop-cast film of H₂OPPP deposited onto a mica substrate and (c) corresponding height profile. UV-vis (d) and fluorescence (e) spectra of drop-cast film of H₂OPPP deposited onto a quartz substrate ($\lambda_{\text{ex}} = 420 \text{ nm}$).

5. Acidochromism studies of H₂DPPP, H₂TPPP and H₂OPPP in chloroform solution

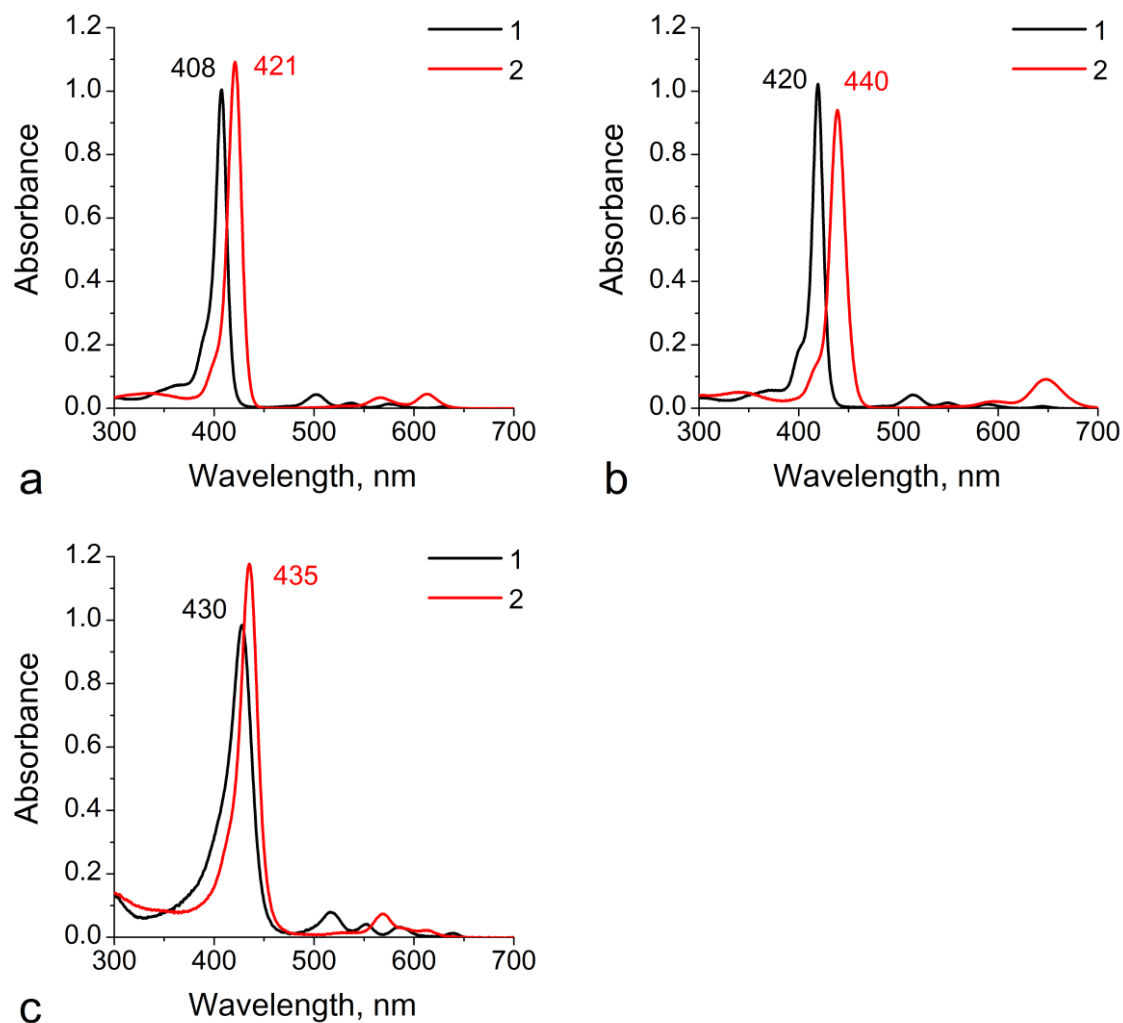
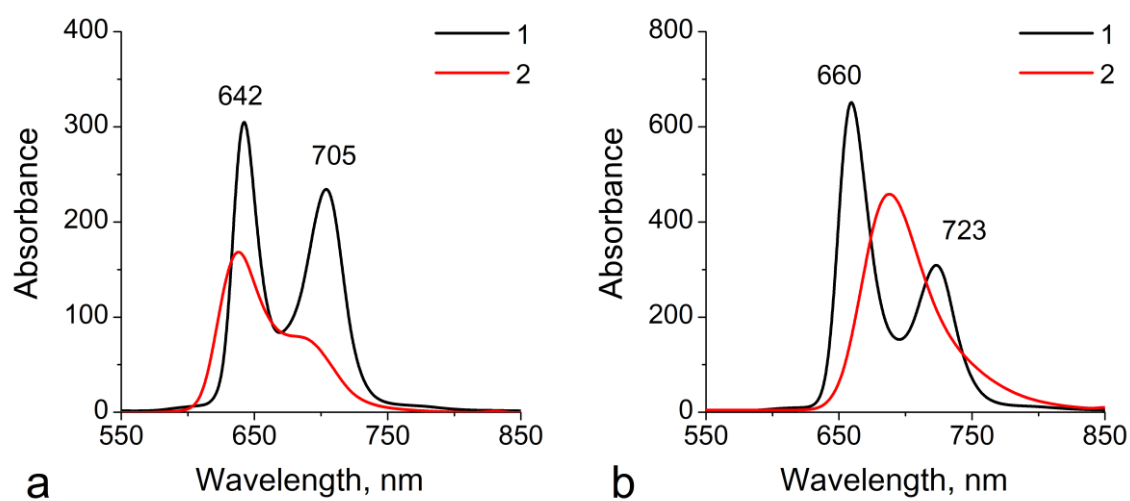


Figure S8. UV-vis spectra of H₂DPPP (a), H₂TPPP (b) and H₂OPPP (c) in chloroform solution (1) upon addition of TFA (2).



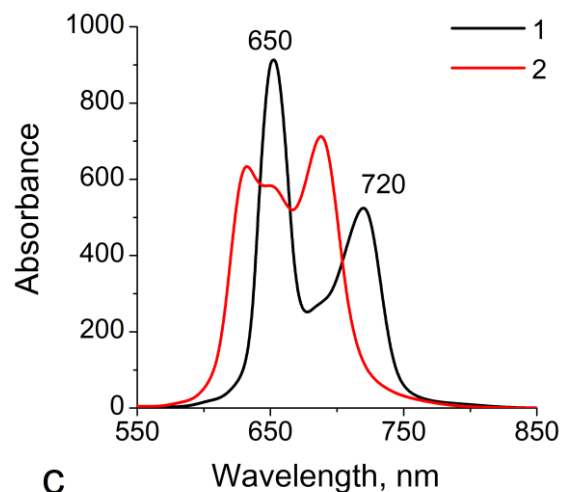


Figure S9. Fluorescence spectra of H₂DPPP (a), H₂TPPP (b) and H₂OPPP (c) in chloroform solution (1) upon addition of TFA (2) ($\lambda_{\text{ex}} = 410, 420$ and 430 nm).

6. Monolayers of NiOPPP and ZnOPPP at the air–water interface

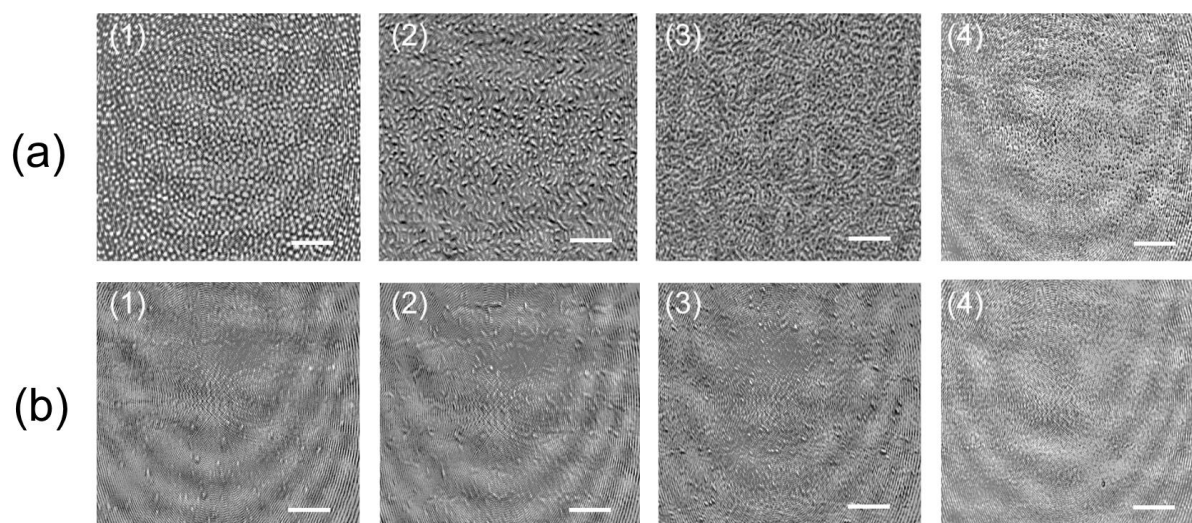


Figure S10. BAM images of the NiOPPP (a) and ZnOPPP (b) monolayers on the aqueous subphase at surface pressure 5 (1), 14 (2), 18 (3) and 22 (4) mN m^{-1} . The scale bar represents $40 \mu\text{m}$.

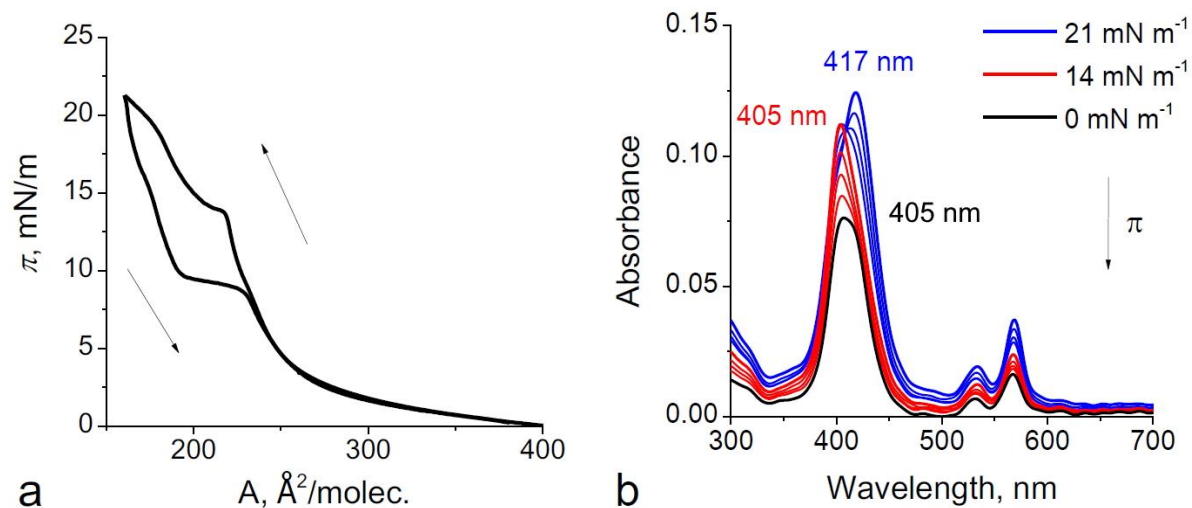


Figure S11. (a) Compression–expansion cycles for porphyrin NiOPPP. (b) *In situ* UV–vis spectra of the NiOPPP monolayer recorded during the monolayer expansion.

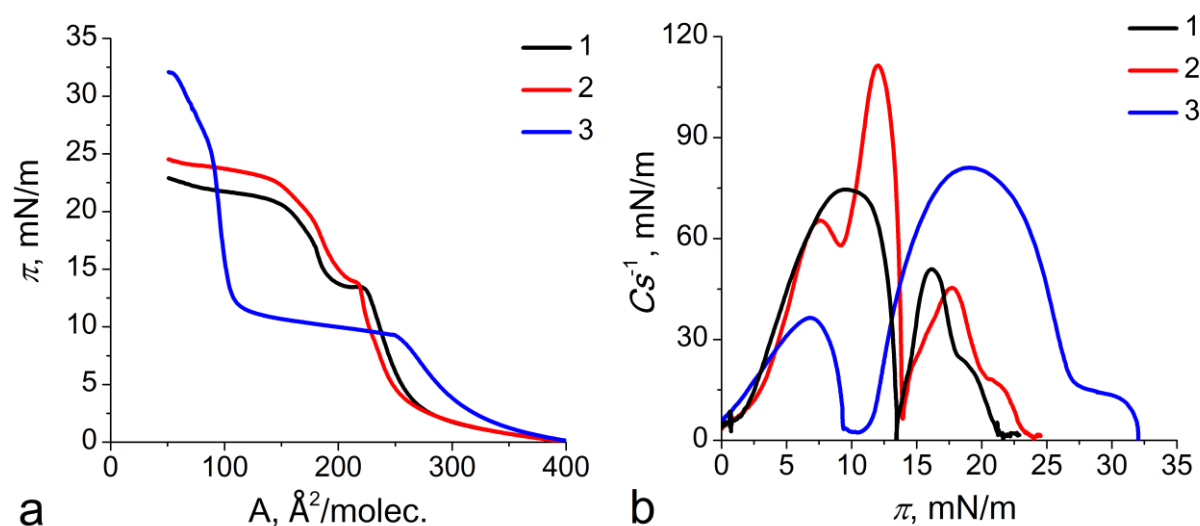


Figure S12. (a) Surface pressure–area isotherms and (b) compressibility modulus C_s^{-1} vs. surface pressure plots for the H₂OPPP (1), NiOPPP (2) and ZnOPPP (3) monolayers on the water surface.

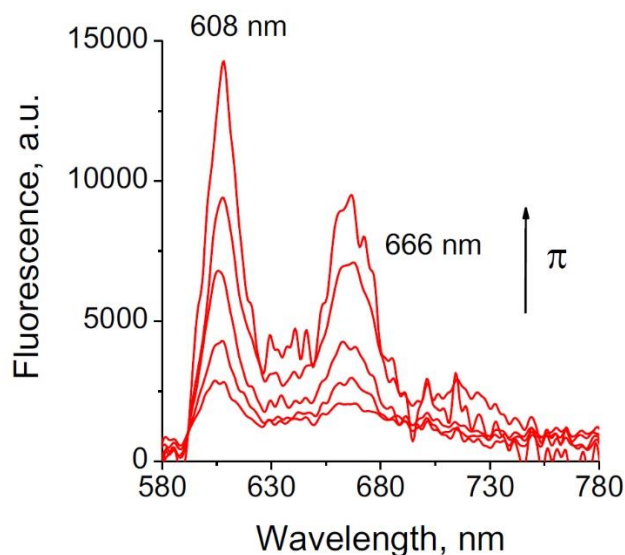


Figure S13. *In situ* fluorescence spectra ZnOPPP monolayer on the deionized water surface. *In situ* fluorescence spectra are recorded during the monolayer compression ($\lambda_{\text{ex}} = 440 \text{ nm}$).

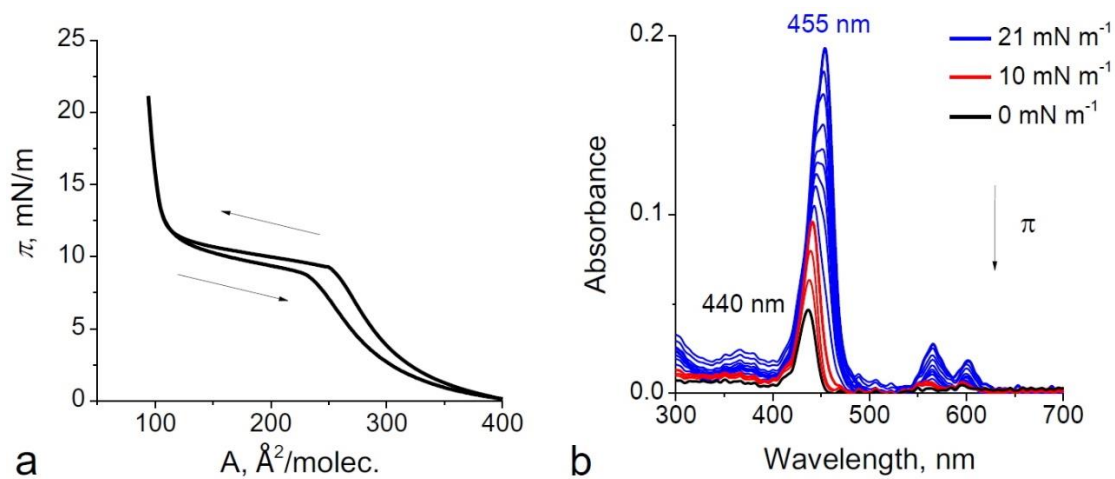


Figure S14. (a) Compression–expansion cycles for porphyrin ZnOPPP. (b) *In situ* UV–vis spectra of the ZnOPPP monolayer recorded during the monolayer expansion.

7. LS films of NiOPPP and ZnOPPP

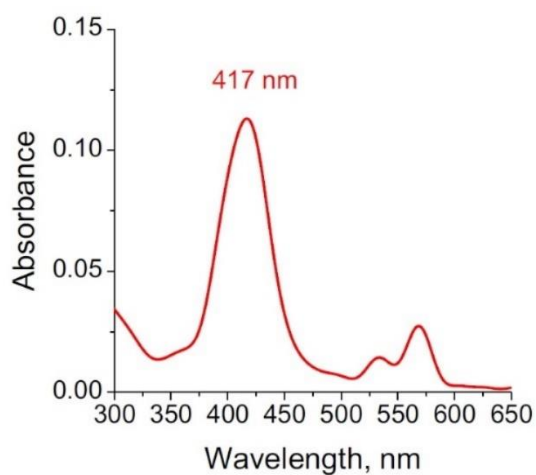


Figure S15. UV-vis spectra of one-layer LS film NiOPPP deposited onto a PVC substrate at a surface pressure of 18 mN m^{-1} .

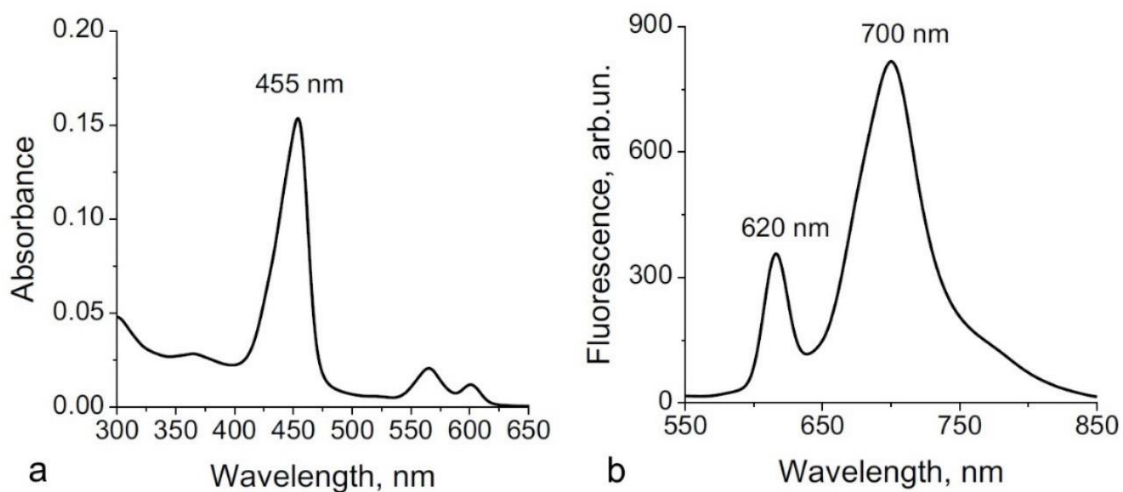


Figure S16. UV-vis (a) and fluorescence (b) spectra of one-layer LS film of ZnOPPP deposited onto a PVC substrate at a surface pressure of 18 mN m^{-1} , ($\lambda_{\text{ex}} = 440 \text{ nm}$).

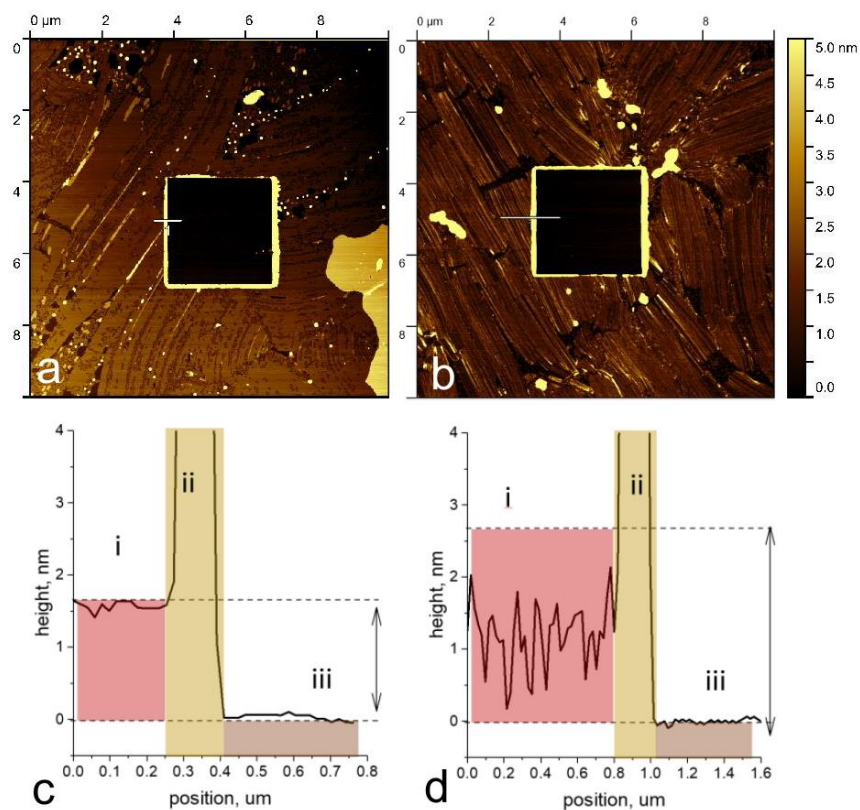


Figure S17. AFM images obtained after ‘scratching’ the samples in contact mode to reveal bare mica: one-layer LS films of NiOPPP (a) and ZnOPPP (b) transferred onto mica substrates at a surface pressure of 18 mN m^{-1} . (c, d) Corresponding height profiles obtained along the scratched surface line for samples transferred. Colored regions on the height profiles correspond to (i) observed porphyrin domains, (ii) film material piled up after ‘scratching’, and (iii) bare mica surface.

8. Monolayer and LS film of ZnTPP

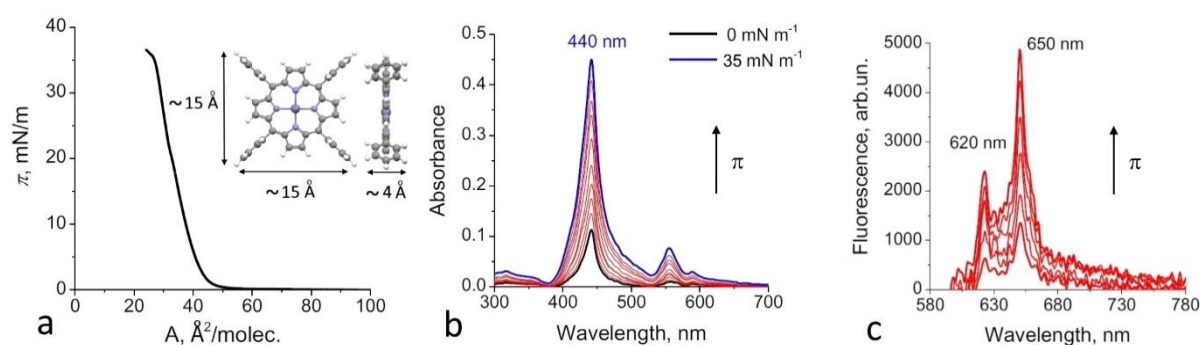


Figure S18. Surface pressure vs area isotherm (a), *in situ* UV-vis (b) and fluorescence spectra (c) of ZnTPP monolayer on the deionized water surface. Insets: Spacefill model of ZnTPP (a) molecule optimized by the semi-empirical PM6 method. *In situ* UV-vis and fluorescence spectra are recorded during the monolayer compression ($\lambda_{\text{ex}} = 440 \text{ nm}$).

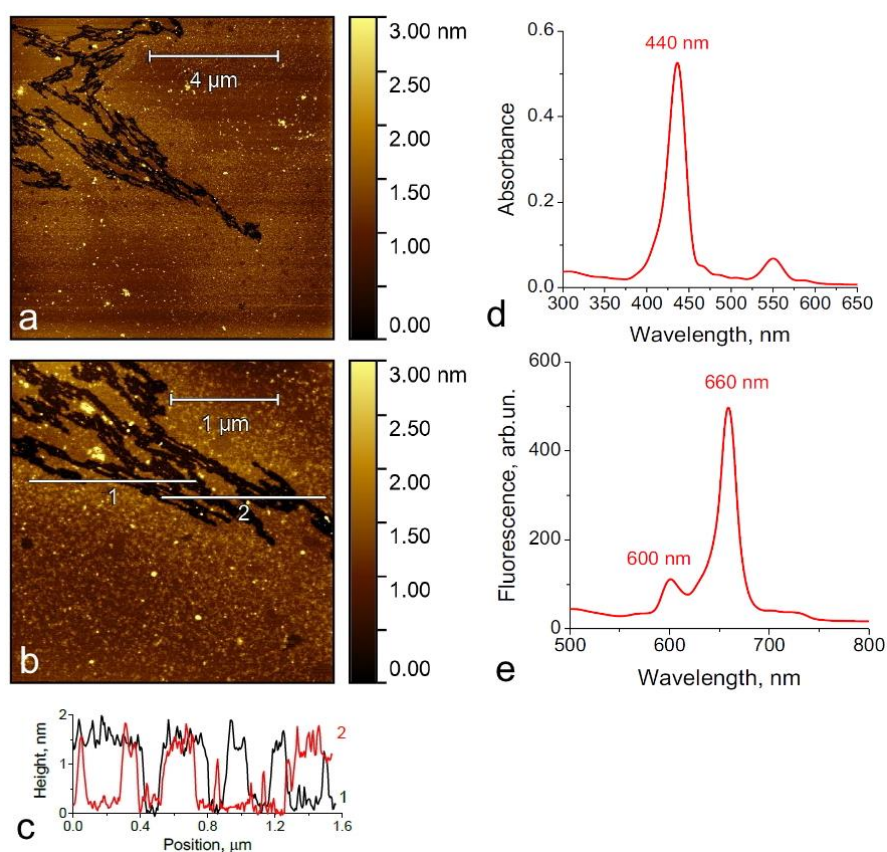


Figure S19. (a, b) AFM images of one-layer LS films of ZnTPP deposited onto a mica substrate at 18 mN m^{-1} from the deionized water surface and (c) corresponding height profiles. UV-vis (d) and fluorescence (e) spectra of one-layer LS film of ZnOPPP deposited onto a PVC substrate at a surface pressure of 18 mN m^{-1} , ($\lambda_{\text{ex}} = 440 \text{ nm}$).

9. UV-vis and fluorescence spectroscopies studies of ZnOPPP and ZnTPP in chloroform solutions in presence of amines

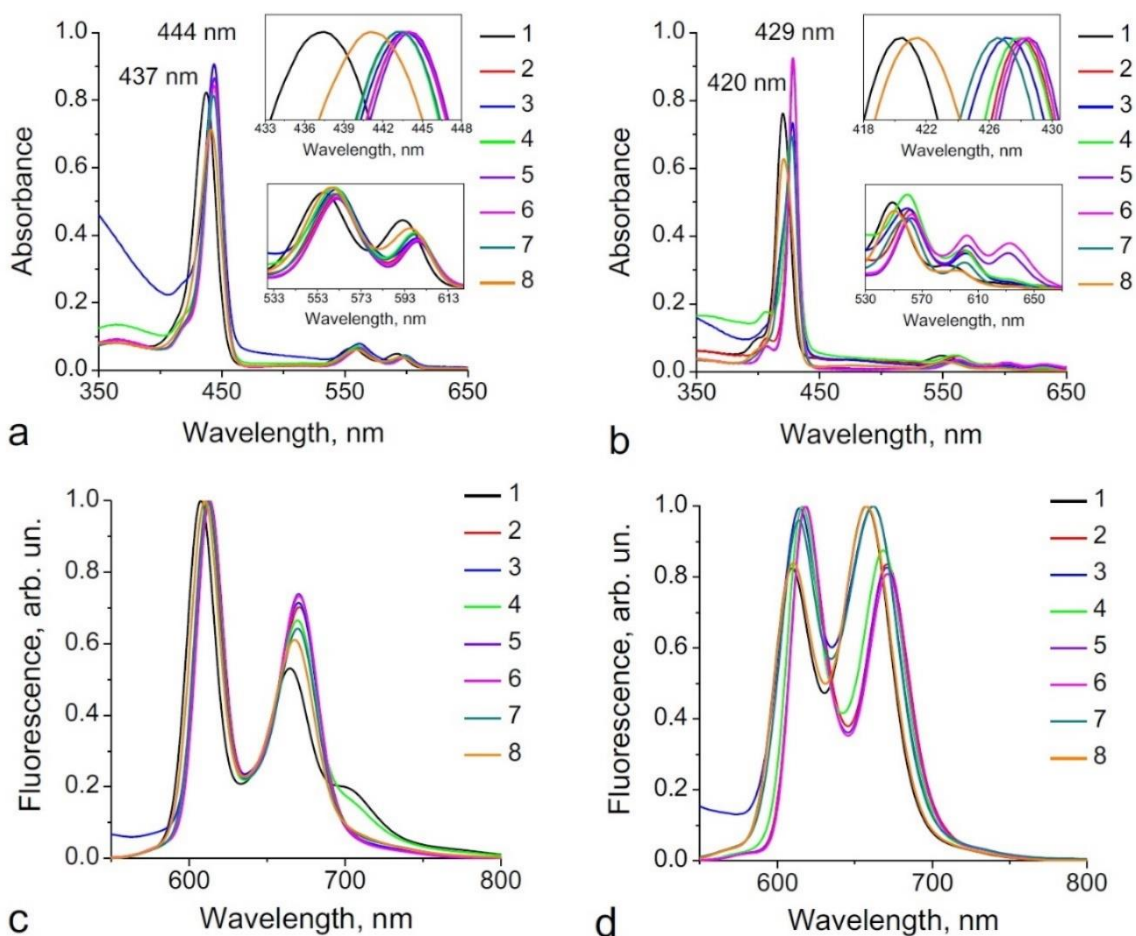


Figure S20. UV-vis (a, b) and fluorescence (c, d) spectra ($\lambda_{\text{ex}} = 440 \text{ nm}$) of ZnOPPP (a, c, 1) and ZnTPP (b, d, 1) chloroform solutions ($6.25 \mu\text{M}$) in presence of pyridine (2), triethylamine (3), aniline (4), diethylamine (5), benzylamine (6), trimethylpyridine (7), diisopropylamine (8) ($5 \mu\text{L}$ of each amine was added into porphyrin solutions).

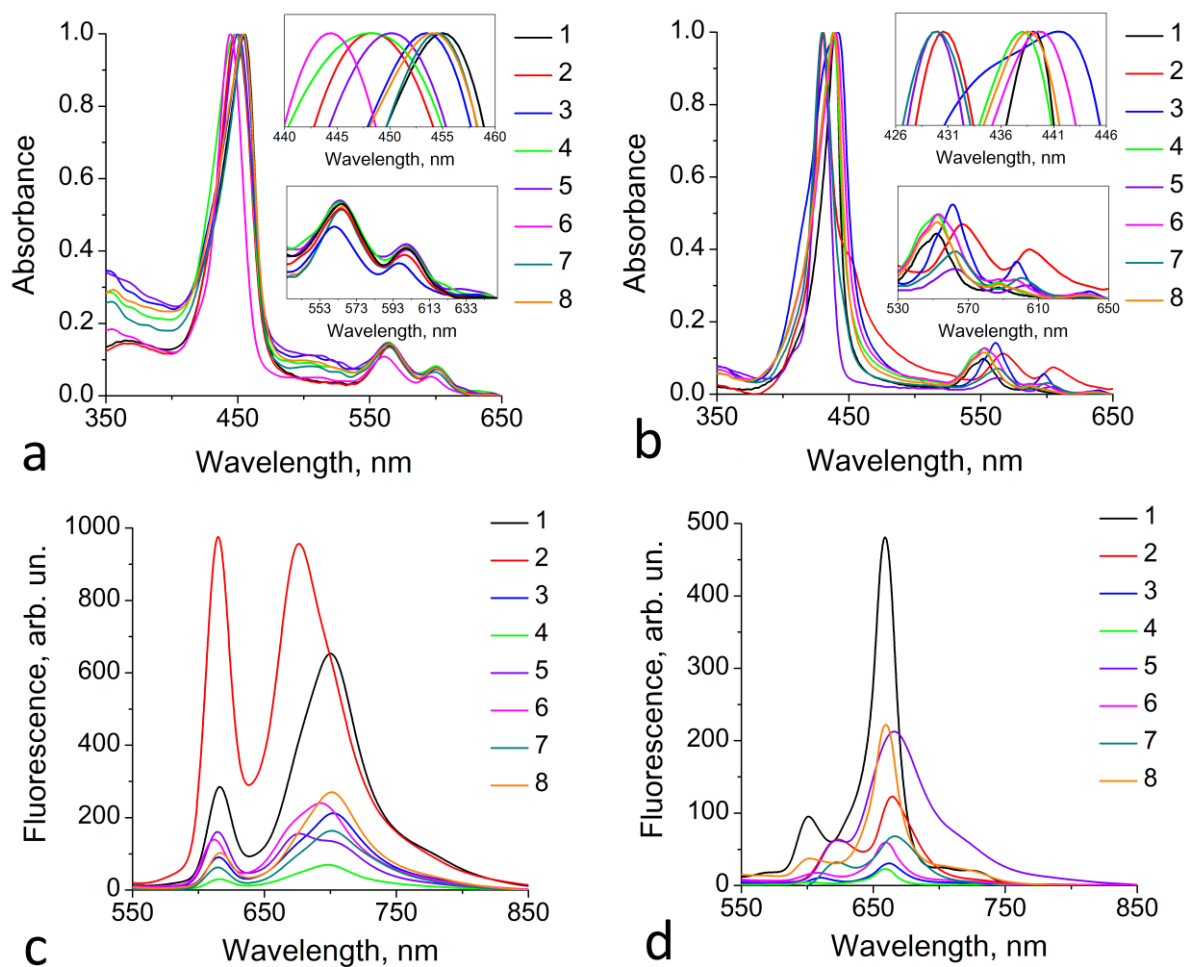


Figure S21. Normalized UV-vis (a, b) and fluorescence (c, d) spectra ($\lambda_{\text{ex}} = 440 \text{ nm}$) of one-layer LS films of ZnOPPP (a, c, 1) and ZnTPP (b, d, 1) deposited onto a PVC at 18 mN m^{-1} from the deionized water and treated by pyridine (2), triethylamine (3), aniline (4), diethylamine (5), benzylamine (6), 2,4,6-trimethylpyridine (7), diisopropylamine (8) vapors for 1 min.

10. Quantum yield measurements for ZnOPPP LS film

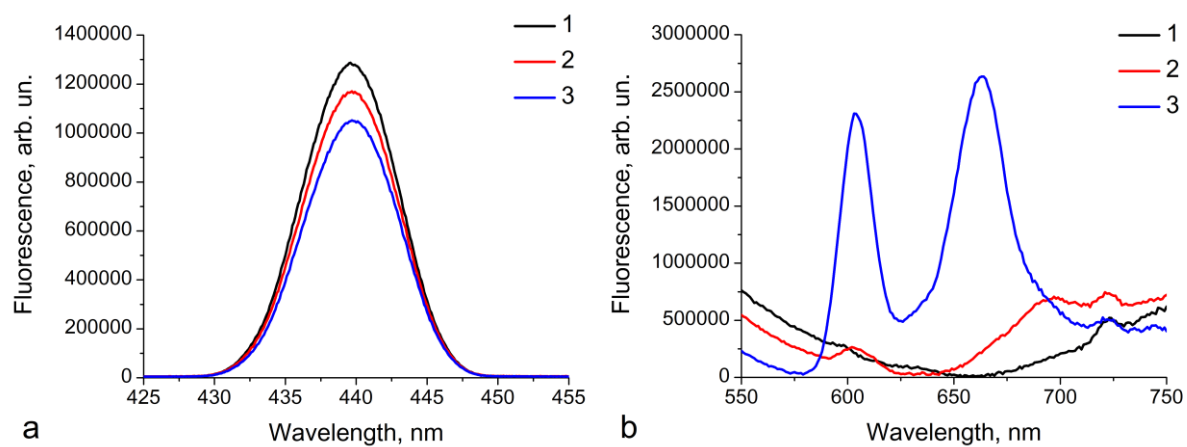


Figure S22. Fluorescence spectra ($\lambda_{\text{ex}} = 440$ nm) of laser excitation beam (a) and samples (b): PVC substrate (1), one-layer ZnOPPP LS films before (2) and after treatment by pyridine vapor for 60 s (3).